Turkish Journal of Electrical Engineering & Computer Sciences

http://journals.tubitak.gov.tr/elektrik/

Research Article

Turk J Elec Eng & Comp Sci
(2017) 25: 4768 – 4776

doi:10.3906/elk-1702-98

A novel empirical SIR-to-CQI mapping rule for DC-HSDPA systems

Çetin KURNAZ[1,*], **Begüm KORUNUR ENGİZ**[1], **Murat Oğuz ESENALP**[2]
[1]Department of Electrical and Electronics Engineering, Faculty of Engineering, Ondokuz Mayıs University, Samsun, Turkey
[2]Turkcell Communication and Technology Company, Samsun, Turkey

Received: 08.02.2017 • **Accepted/Published Online:** 15.09.2017 • **Final Version:** 03.12.2017

Abstract: This study aims to determine the mapping rule for signal-to-interference ratio (SIR) to channel quality indicator (CQI) based on DC-HSDPA real field measurements. The measurements were performed using the TEMS Investigation Tool at 85 different propagation mediums. The measurement results showed that the SIR-to-CQI mapping methods in the literature were insufficient to characterize actual radio environments; thus, proposal of a new empirical SIR-to-CQI mapping rule was aimed. This rule provides substantially better performance than the existing methods, and with this rule CQI can be generated from SIR with an accuracy of around 90% for DC-HSDPA systems.

Key words: DC-HSDPA, channel quality indicator, SIR-to-CQI mapping, TEMS Investigation Tool

1. Introduction

High Speed Packet Access (HSDPA) technology is defined by Release-5 of the 3GPP (3rd Generation Partnership Project) UMTS standard. In this technology, shorter transmit time interval (TTI); adaptive modulation and coding (AMC), in which the modulation scheme and coding rate are adaptively changed according to the downlink channel quality; fast retransmission using hybrid automatic repeat requests; and new physical channels help to achieve higher data rates [1,2]. The 3GPP developed Release-8, named dual carrier HSDPA (DC-HSDPA), to eliminate destructive effects of frequency selectivity of the channel on high data rate communication [3]. In DC-HSDPA, up to 42 Mbps data rates are achievable with the simultaneous use of two adjacent 5 MHz HSDPA carriers. DC-HSDPA mainly improves the user's individual throughput, while overall system capacity remains the same [4–9]. In HSDPA-based systems, downlink channel conditions are defined by the CQI values. These values are reported by user equipment (UE) to the base station (Node-B) in each 2 ms. According to the CQI value, Node-B adapts the next transport block size (TBS), modulation scheme, and number of channelization codes dynamically. CQI is a key indicator determining the downlink channel quality and is closely related to AMC accuracy and maximum throughput. Thus, it is crucial to generate the correct CQI values that describe the real channel conditions.

2. SIR-to-CQI mapping methods

In HSDPA the CQI varies within the range of 1–30 depending on many factors. The main factors are the distance of UE from Node-B, transmission power, and fading. The higher the CQI value, the better channel conditions

*Correspondence: ckurnaz@omu.edu.tr

are. It is possible to achieve higher data rates by using a larger TBS and a higher modulation index (i.e. 64QAM). The channel's destructive effect is decreased by using more robust modulation schemes (i.e. QPSK) at lower CQI. The CQI value is determined by the UE depending on its brand and model, considering the SIR value and a less than 10% block error rate (BLER) [10]. In order to obtain the highest system performance, the exact CQI values must be determined. If CQI were to be estimated as higher than it actually is, many bits would be received inaccurately due to a larger TBS and system performance would decrease. However, if the CQI is lower than its real value, channel capacity cannot be used effectively, causing the throughput to decrease. Thus, determining the most appropriate CQI value is necessary to maximize throughput. There have been several studies [11–29] on SIR or SINR (signal-to-interference plus noise ratio) and CQI in a HSDPA system, but only a few of them [25–29] focused on SIR-to-CQI mapping methods for a HSDPA system. In [25] SINR-to-CQI mapping is defined for an AWGN channel, and the linear relation between them is determined for a BLER of 0.1. The authors of [26] also performed AWGN simulations to derive the relation between SINR and CQI that is approximated through a linear function. A novel SIR-to-CQI mapping method that satisfies the 3GPP requirements was proposed in [27]. The performance of the proposed mapping method was verified via the link level simulator for ITU channels. The work in [28] also proposed a novel mapping method that helps to achieve optimum throughput for ITU propagation channels. In [29] the calculation of SIR of a HSDPA system was performed through the analysis of CQI and simulations. However, there are no studies on a DC-HSDPA system. Moreover, the studies [25–29] given in Table 1 investigated the SIR-to-CQI mapping methods for AWGN and ITU test channels; so far there have not been any assessments based on real field measurements. This study aims to propose a novel SIR-to-CQI mapping method that represents the exact DC-HSDPA service environment based on real field measurements.

3. DC-HSDPA system measurements

In this study, DC-HSDPA field measurements were carried out in different propagation environments in Samsun, Turkey, by using the TEMS Investigation Tool, version 12.1.

The air interface between the UE and Node-B for many wireless technologies including HSDPA, WiMAX, and LTE can be tested by using the TEMS Investigation Tool. The measurements were performed at 2114.7 MHz carrier frequency with the total transmitter power of Node-B being 44.7 dBm and a fixed user location using a HUAWEI E372 double carrier modem. The mentioned modem is in category 24 and uses QPSK modulation for CQI values in the range of 1–15, 16-QAM in the range of 16–25, and 64-QAM in the range of 26–30 in accordance with 3GPP standards [30]. Data were collected in 85 different fully surrounded environments during the download process of a 100 MB data file. During measurements received power (received signal code power, RSCP), CQI, user throughput, and SIR, which is the ratio of energy in the DPCC (dedicated physical control channel) to that of the interference and noise received by the UE, were recorded. Measurement routes are shown in Figure 1. In Figure 1, each cyan dot corresponds to a rough fixed unique UE location; the yellow line represents the route; the white star represents Node-B. Additional details of the measurements can be found in [31].

4. Analysis and results

In the measurements, the location that yields the highest throughput is named Ch1. The changes in received power, SIR, CQI, and user throughput versus time for Ch1 are shown in Figure 2. Since the signal reception power is high for Ch1 (between –34 dBm and –50 dBm), the measured SIR value is also high, measuring

Figure 1. Measurement routes for different environments.

between 14 dB and 27 dB with an average value of 20.71 dB. As a result of a high SIR value, high CQI values are obtained, varying between 28 and 30. As seen in Figure 2, according to variations in channel conditions the SIR value also changes and results in a change of CQI value. Because of the CQI value, 100 MB of data was downloaded in 38.5 s using 64-QAM. Meanwhile, the highest throughput was 23.1 Mbps and the average throughput was 20.9 Mbps for Ch1.

Similar measurements were conducted at the remaining 84 locations, and the collected data were then assessed. In order to eliminate sharp discontinuities in the data, the *smooth* function in MATLAB was used for smoothing and the span and the method of the function were chosen as *0.1* and *rloess*, respectively. The changes in average SIR and CQI values for all measurement locations are shown in Figure 3a, while the measured CQI values versus SIR are given in Figure 3b. Figure 3a shows how the increase in SIR causes an increment in CQI and vice versa. These parameters can be related mathematically, as follows:

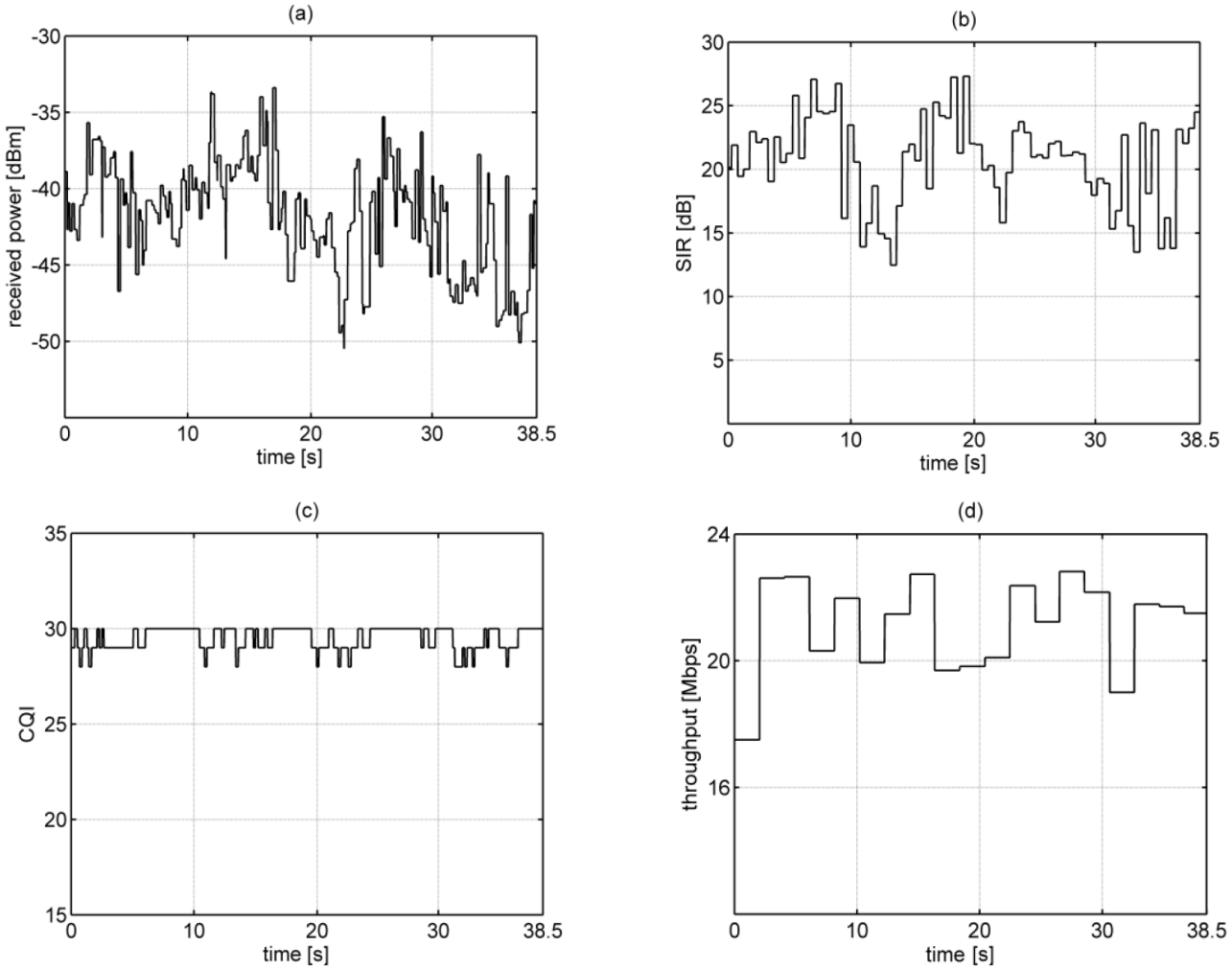

Figure 2. a) Received power, b) SIR, c) CQI, d) user throughput for Ch1.

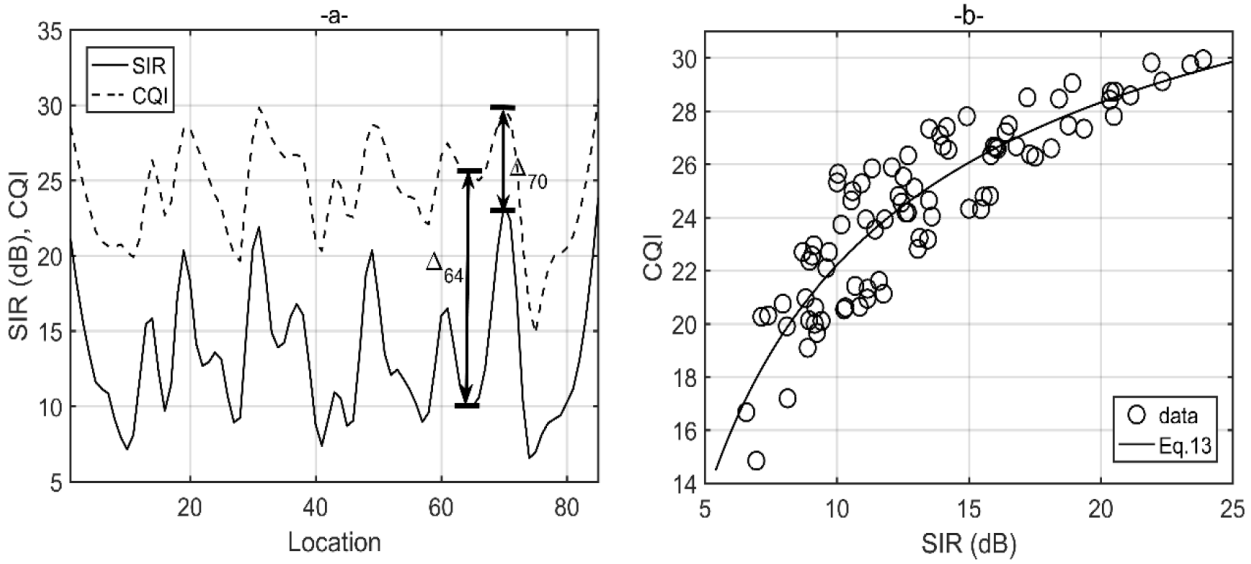

Figure 3. a) SIR and CQI values versus location, b) CQI versus SIR.

$$CQI_i = SIR_i + \Delta_i, \tag{1}$$

where CQI_i is the measured CQI value, SIR_i is the measured SIR value, and Δ_i is the relative change for the ist UE location.

However, Δ_i is not the same for all locations. For example, the maximum relative change is $\Delta_{64} = 15.61$, while the minimum relative change is $\Delta_{70} = 6.36$. The mean of the relative change is 11.01.

Using the mean of the relative change gives rise to a new mathematical expression for the generated CQI (CQI_p), as follows:

$$CQI_p = SIR + 11.01. \tag{2}$$

The accuracy of the method is evaluated in terms of normalized root mean squared error (NRMSE), as given in Eq. (3):

$$NRMSE = \frac{\sqrt{\frac{1}{n}\sum_{i=1}^{n}(CQI_i - CQI_p)^2}}{\max(CQI) - \min(CQI)}, \tag{3}$$

where i is measurement location and n is total measurement locations.

The NRMSE of the method from Eq. (2) is 0.1374. The mapping methods given in Table 1 in [25–29] are applied to measured data, and the NRMSEs are calculated and given in Table 2.

Table 1. Mapping rules in the literature.

Mapping rule	Reference
$CQI = SINR + 4.5$	[25]
$CQI = \begin{cases} 0 & SINR \le -3.96 \\ \frac{SINR}{1.02} + 4.81 & -3.96 < SINR < 26.04 \\ 30 & 26.04 \le SINR \end{cases}$	[26]
$CQI = \begin{cases} 14.004686135 + 0.640014549(SIR) & SIR \ge 20 \\ 5.249450552 + 1.07142637(SIR) & SIR < 20 \end{cases}$	[27]
$CQI = \begin{cases} SINR + 2.5 & SINR < 6 \\ SINR + 3.0 & 6 \le SINR \le 10.5 \\ SINR + 3.5 & SINR > 10.5 \end{cases}$	[28]
$CQI = 10\log(SIR) + 4.5$	[29]

Since the NRMSE values are very high, even higher than Eq. (2), these methods are insufficient for estimating CQI values for real-time systems. When using these methods, channel capacity cannot be used efficiently and the maximum achievable throughput cannot be reached. Therefore, a more accurate novel SIR-to-COI mapping method must be proposed, which is very crucial in DC-HSDPA systems. In order to clarify the relationship between SIR and CQI, commonly used curve-fitting methods (i.e. power, polynomial, exponential, rational) are applied to data. The purpose of curve-fitting is to find a function, f(x), that minimizes the residual and the distance between the data samples (y_i) and f(x). The relation between the dependent variables y_i and

Table 2. The NRMSEs of previous studies [25–29].

Reference	NRMSE
[25]	0.4397
[26]	0.4357
[27]	0.3436
[28]	0.5115
[29]	0.3705

the independent variable x_i is given in Eq. (4):

$$y_i = f(a, b; x_i) + e_i \quad i = 1, 2, ..., n, \tag{4}$$

where a and $b$are the curve-fitting coefficients, x_i is the SIR value at the ith location, and $e_i$is the error for the ith data point as defined by the following:

$$e_i = f(a, b; x_i) - y_i. \tag{5}$$

The sum of the square of the errors (SEE) is given in Eq. (6):

$$SSE = \sum_{i=1}^{n} e_i^2 = \sum_{i=1}^{n} [f(a, b; x_i) - y_i]^2. \tag{6}$$

The unknowns a and b can be determined by minimizing the SEE. In order to do this, the partial derivatives of the SEE with respect to a and b are set to zero. The calculation process is given only for the rational method, since the other methods' NRMSEs are higher. The partial derivative of the rational method is as follows:

$$\frac{\partial SEE}{\partial a} = ax_i^2 - bx_i y_i - x_i^2 y_i = 0, \quad \frac{\partial SEE}{\partial b} = -ax_i y_i + by_i^2 + x_i y_i^2 = 0. \tag{7}$$

If matrix notation is used, a and b can be calculated using Eq. (8):

$$\begin{bmatrix} \sum_{i=1}^{n} x_i^2 & \sum_{i=1}^{n} -x_i y_i \\ \sum_{i=1}^{n} -x_i y_i & \sum_{i=1}^{n} y_i^2 \end{bmatrix} \begin{bmatrix} a \\ b \end{bmatrix} = \begin{bmatrix} \sum_{i=1}^{n} x_i^2 y_i \\ \sum_{i=1}^{n} -x_i y_i^2 \end{bmatrix},$$

$$\begin{bmatrix} a \\ b \end{bmatrix} = \begin{bmatrix} \sum_{i=1}^{n} x_i^2 & \sum_{i=1}^{n} -x_i y_i \\ \sum_{i=1}^{n} -x_i y_i & \sum_{i=1}^{n} y_i^2 \end{bmatrix}^{-1} \begin{bmatrix} \sum_{i=1}^{n} x_i^2 y_i \\ \sum_{i=1}^{n} -x_i y_i^2 \end{bmatrix}. \tag{8}$$

The a and b values that yield the minimum SEE are obtained by using Eq. (6) for polynomial, exponential, power, and rational curve-fitting methods. The CQI_p and the NRMSEs are given in Table 3. As seen in Table 3, the rational curve-fitting method yields the minimum NRMSE value of 0.0991 and produces the best fit. The NRMSE value obtained by using the proposed rational equation (Eq. (3)) is approximately 3.4 times lower than

Table 3. NRMSE performances of the curve-fitting methods.

Curve-fitting method		CQI_p = f(a,b;SIR)	NRMSE	
Polynomial	$f(a,b;x_i) = a + bx_i$	$CQI_p = 15.37 + 0.6734(SIR)$	0.1067	(9)
Exponential	$f(a,b;x_i) = ae^{bx_i}$	$CQI_p = 17.14e^{0.0259(SIR)}$	0.1113	(10)
Power	$f(a,b;x_i) = ax_i^b$	$CQI_p = 9.307(SIR)^{0.3757}$	0.1002	(11)
Rational	$f(a,b;x_i) = \frac{ax_i}{b+x_i}$	$CQI_p = \frac{36.603(SIR)}{6.1212+(SIR)}$	0.0991	(12)

the one in [27]. Because of being proposed on the basis of real-time link-level network results, the rule yields much lower NRMSE values than the others. Therefore, the actual radio environment can be best determined by using the proposed equation and the channel capacity can be improved.

As mentioned above, many frequently used fitting methods were applied; for the sake of brevity, the four best results and corresponding methods are provided in this study. However, forgoing complexity allows one to have lower NRMSEs, which is possible by using more coefficients in the previously mentioned methods. For this purpose, additional analyses were performed for the listed methods with more coefficients. The method among them that yielded the minimum NRMSE of 0.0966 is as shown in Eq. (13), and the generated CQI values obtained through Eq. (13) are illustrated in Figure 3b.

$$CQI_p = -67.91(SIR)^{-0.539} + 41.84 \tag{13}$$

Analyses show that using more coefficients does not lead to significant improvement in NRMSE when compared with Eq. (3) (0.0991). It is concluded from the NRMSEs that if complexity is important one should use Eq. (3). Otherwise, Eq. (13) may be preferred for mapping with lower NRMSE values. However, using Eq. (13), CQI values can be determined with 90% accuracy. Despite giving better NMRSEs than the literature, there is still 10% inaccuracy, and one parameter-mapping rule may not be considered as sufficient enough for determining CQI for a real-time DC-HSDPA system.

5. Conclusions

In this study, a novel empirical SIR-to-CQI mapping rule based on real field measurements is proposed for a DC-HSDPA system. It is shown that the proposed method yields approximately 3.4 times lower NRMSE than in [27]. With the proposed method, CQI values, which represent actual radio environments, can be determined with an accuracy of about 90% and higher throughput can be achieved with the efficient use of channel capacity. The precision of the proposed equation can be increased with the use of extra channel parameters apart from SIR.

References

[1] Holma H, Toskala A. HSDPA/HSUPA for UMTS. 1st ed. London, UK: John Wiley & Sons Ltd., 2006.

[2] Dahlman E, Parkvall S, Skold J, Beming P. 3G Evolution: HSPA and LTE for Mobile Broadband. 2nd ed. Oxford, UK: Academic Press, 2008.

[3] 3rd Generation Partnership Project. 3GPP TS 25.211. V8.7.0. Physical channels and mapping of transport channels onto physical channels (FDD). Sophia Antipolis, France: 3GPP, 2010.

[4] Johansson K, Bergman J, Gerstenberger D, Blomgren M, Wallen A. Multi-carrier HSDPA evolution. In: IEEE 69th Vehicular Technology Conference (VTC Spring); 26–29 April 2009; Barcelona, Spain. New York, NY, USA: IEEE. pp. 1-5.

[5] deAndrade DM, Klein A, Holma H, Viering I, Liebl G. Performance evaluation on dual-cell HSDPA operation. In: IEEE 70th Vehicular Technology Conference (VTC Fall); 20–23 September 2009; Anchorage, AK, USA. New York, NY, USA: IEEE. pp. 1-5.

[6] Zhang D, Vitthaladevuni PK, Mohantary B, Hou J. Performance analysis of dual-carrier HSDPA. In: IEEE 71st Vehicular Technology Conference (VTC Spring); 16–19 May 2010; Taipei, Taiwan. New York, NY, USA: IEEE. pp. 1-5.

[7] Mohan S, Kapoor R, Mohanty B. Dual cell HSDPA application performance. In: IEEE 73rd Vehicular Technology Conference (VTC Spring); 15–18 May 2011; Budapest, Hungary. New York, NY, USA: IEEE. pp. 1-6.

[8] Esenalp M, Kurnaz Ç. Performance evaluation of dual carrier HSDPA in indoor environment. In: IEEE 21st Signal Processing and Communications Applications; 24–26 April 2013; North Cyprus. New York, NY, USA: IEEE. pp. 1-4.

[9] Oh J, Hwang JY, Han Y. Efficient carrier selection schemes for dual-carrier HSDPA system. In: 17th Asia-Pacific Conference on Communications; 3–5 October 2011; Sabah, Malaysia. New York, NY, USA: IEEE. pp. 79-83.

[10] Sesia S, Toufik I, Baker M. LTE: The UMTS Long Term Evolution from Theory to Practice. 2nd ed. Chichester, UK: Wiley, 2011.

[11] Deng R, Liu G, Yang J. Utility-based optimized cross-layer scheme for real-time video transmission over HSDPA. IEEE T Multimedia 2015; 9: 1495-1507.

[12] Elnashar A, El-Saidny MA. Looking at LTE in practice: a performance analysis of the LTE system based on field test results. IEEE Veh Technol Mag 2013; 81-92.

[13] Huang CY, Chung WC, Chang CJ, Ren FC. An intelligent HARQ scheme for HSDPA. IEEE T Veh Technol 2011; 4: 1602-1611.

[14] Mehlführer C, Caban S, Rupp M. Measurement-based performance evaluation of MIMO HSDPA. IEEE T Veh Technol 2010; 9: 4354-4367.

[15] Bruin DI, Brouwer F, Whillans N, Fu Y, Xiao Y. Performance analysis of hybrid ARQ characteristics in HSPA. Wireless Pers Commun 2007; 42: 337-353.

[16] Mutairi A, Baroudi U. An adaptive CQI-based algorithm for HSDPA flow control. Arab J Sci Eng 2013; 38: 2357-2365.

[17] Liyanage NDK, Abeywickrama CA, Kumari PMIU, De Silva SA, Wavegedara CB. Performance investigation of hybrid ARQ in HSDPA systems with AMC. In: Moratuwa Engineering Research Conference (MERCon); 5–6 April 2016; Moratuwa, Sri Lanka. pp. 126-131.

[18] Kelch L, Pögel T, Wolf L, Sasse A. CQI maps for optimized data distribution. In: IEEE 78th Vehicular Technology Conference (VTC Fall); 2–5 September 2013; Las Vegas, NV, USA. New York, NY, USA: IEEE. pp. 1-5.

[19] Ito A, Shimizu M. Channel estimation for SIR measurement in HSDPA systems. In: IEEE 66th Vehicular Technology Conference (VTC Fall); 30 September–3 October 2007; Baltimore, MD, USA. New York, NY, USA: IEEE. pp. 1012-1016.

[20] Isotalo T, Lempiäinen J. HSDPA measurements for indoor DAS. In: IEEE 65th Vehicular Technology Conference (VTC Spring); 22–25 April 2007; Dublin, Ireland. New York, NY, USA: IEEE. pp. 1127-1130.

[21] Iizuka Y, Nakamori T, Ishii H, Tanaka S, Ogawa S, Ohno K. Field experiment results of user throughput performance in WCDMA HSDPA. In: IEEE 16th International Symposium on Personal, Indoor and Mobile Radio Communications (PIMRC); 11–14 September 2005; Berlin, Germany. New York, NY, USA: IEEE. pp. 346-351.

[22] Klockar L, Simonsson A, Gunnarsson F, Borg A. Channel characterization and HSDPA bit rate prediction of a dense city network. In: IEEE 69th Vehicular Technology Conference (VTC Spring); 26–29 April 2009; Barcelona, Spain. New York, NY, USA: IEEE. pp. 1-5.

[23] Kim J, Hong YJ, Sung KD. A radio channel estimation scheme using the CQI feedback information in high speed downlink packet access. In: IEEE International Conference on Communications; 11–15 June 2006; İstanbul, Turkey. New York, NY, USA: IEEE. pp. 5754-5759.

[24] Touheed H, Quddus AU, Tafazolli R. An improved link adaptation scheme for high speed downlink packet access. In: IEEE 67th Vehicular Technology Conference (VTC Spring); 11–14 May 2008; Singapore. New York, NY, USA: IEEE. pp. 2051-2055.

[25] Motorola and Nokia. Revised CQI Proposal. 3GPP RAN WG1 Technical Report. R1-02-0675. Chicago, IL, USA: Motorola and Nokia, 2002.

[26] Brouwer F, Bruin I, Silva CS, Souto N, Cercas F, Correia A. Usage of link-level performance indicators for HSDPA network level simulations in E-UMTS. In: IEEE 8th International Symposium on Spread Spectrum Techniques and Applications; 30 August–2 September 2004; Sydney, Australia. New York, NY, USA: IEEE. pp. 844-848.

[27] Ko K, Lee D, Lee M, Lee HS. A novel SIR to channel-quality indicator (CQI) mapping method for HSDPA system. In: IEEE 64th Vehicular Technology Conference (VTC Fall); 25–28 September 2006; Montreal, Canada. New York, NY, USA: IEEE. pp. 1-5.

[28] Freudenthaler K, Springer A, Wehinger J. Novel SIR-to-CQI mapping maximizing the throughput in HSDPA. In: IEEE Wireless Communications and Networking Conference; 11–15 March 2007; Hong Kong. New York, NY, USA: IEEE. pp. 2231-2235.

[29] Qun HQ, Huang D. Channel quality indication (CQI) application in HSDPA simulation. In: International Conference on Wireless Communications Networking and Mobile Computing; 21–25 September 2007; Shanghai, China. New York, NY, USA: IEEE. pp. 1200-1203.

[30] 3rd Generation Partnership Project. 3GPP TS 25.214 V8.9.0. Third Generation Partnership Project; Technical Specification Group Radio Access Network; Physical layer procedures (FDD) (Release 8). Sophia Antipolis, France: 3GPP, 2010.

[31] Kurnaz Ç, Engiz BK, Esenalp M. A novel throughput mapping method for DC-HSDPA systems based on ANN. Neural Comput Appl 2017; 2: 265-274.